SEISMIC RESPONSE OF TANKS AND VIBRATION CONTROL OF THEIR PIPELINES

Rui Carneiro de Barros
Department of Civil Engineering, Faculdade de Engenharia
FEUP, R. Roberto Frias, Porto 4200-465, Portugal,
Email: rcb@fe.up.pt

1. INTRODUCTION

The purpose of this work is to detail some methodologies applied for analysis of the seismic behaviour of existing bottom supported storage tanks and pipelines, under predominantly horizontal seismic actions. Developments on the established finite element method (FEM), permitted to analyse tanks and their liquid contents by two possible approaches: Ritz method coupled with FEM applied to an analytical solution of the tank-liquid system; FEM of the full system by modelling the liquid as a degenerated solid. Both formulations permit to determine seismic response envelopes. Further, some considerations on active control of cylinders by piezoceramic stacks of actuators are outlined, for potential uses in pipelines and tube-like structures.

2. JUSTIFICATION OF RESEARCH THEMATIC

Observed performance of bottom-supported cylindrical liquid storage tanks, during historic 1960's and 1970's earthquakes and during more recent moderate to severe earthquakes of the 1980's and 1990's, indicates that these industrial facilities undergo several types of damages.

Observed damage on tanks during earthquakes, due to liquid sloshing or to deformation of the tanks and/or their foundations, are mainly: buckling of tank wall above base (elephant foot bulge), roof buckling due to failure of inner supporting columns, roof damage by liquid sloshing (overpressure or suction), failure of welding connection between shell and bottom plate, sliding/rocking of tank, foundation failure by differential settlements associated with liquefaction of soils, torsion buckling of tank wall, and failure of connections between piping and tank wall.

During an earthquake, the dynamic fluid pressures developed on the liquid storage tank thin-walls and foundations are of great importance in the tank response, and in their seismic resistant design. They may cause two major tank shell structural instabilities: elephant-foot bulge type of buckling (Figure 1) and diamond buckling by shell-crippling (Figure 2), as explained by Barros [1].

The elephant-foot bulge buckling is an elasto-plastic instability due to plastification of tank shell by the compressive stresses associated with overturning and by the membrane stresses associated with hydrostatic and hydrodynamic pressures. The diamond buckling is an elastic instability due mainly to axial compressive stresses of the walls by internal pressures, but without yielding of the shell wall (membrane stresses smaller than yielding stresses).

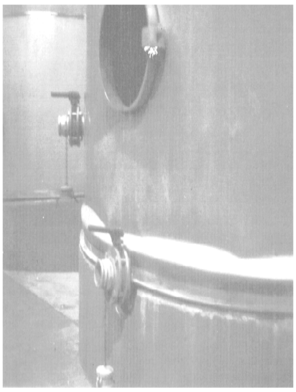

Fig. 1: Elephant-foot bulge

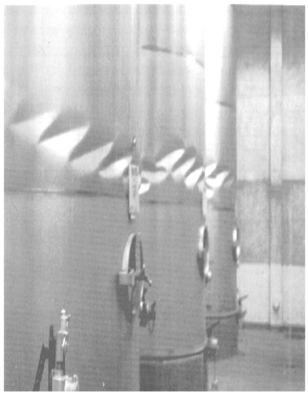

Fig. 2: Diamond buckling

The thematic Seismic Performance and Design of Tanks (and Pipelines) intends to upgrade the design of existing or new bottom supported storage tanks (water, crude oil and energy derivatives, wine, chemicals) and pipelines, under seismic actions (predominantly horizontal) that can cause their total or partial non-functionality.

3. INSTITUTION RECENT EXPERIENCE

The tanks considered herein have either an open top or a roof, and are filled with liquid up to some arbitrary depth of the total shell height. Some past experience on the seismic analysis of metallic tanks by different methodologies has been applied by the author to the study of wine tanks damaged by the San Juan 1977 earthquake, permitting to formulate some reasoning on improvement of general design guidelines. Some more recent experience, through a national R & D project entitled *Seismic Response of Tanks by the Finite Element Method* (FEM), permitted:

- Review comparative studies of distinct rigid/flexible (beam) methodologies for bottom supported tanks, proposed by many authors, accounting (or not) for fluid-structure interaction (FSI);
- Review of rigid tank method complete formulation with all modes (Barros [2,3]);
- Development of tank shell equations by the so-called Sanders theory, as mentioned by Haroun [4] and summarized by Barros [2,3];
- Development of an analytical solution for the boundary value problem (BVP) of the liquid interaction with tank; Use of the least square method, for establishing and approximate shape of deflected boundary, coupled with FEM shell discretization of the tank;
- Successful verification of the methodology through the complete matching of computed results with those of a calibration tank of known elastic responses in the time domain, as mentioned by Haroun [4];
- Development of time history response results of the FSI between tank contained liquid and the FEM model of tank shell, namely for: hydrodynamic pressure, tank stress resultants, generalized displacements, surface elevation, base shears and base moments, as presented by Barros [5];

- Determination of seismic response envelopes for any given bottom supported tank, under Portuguese seismic standards RSAEEP (soil type I, zone A), as presented by Barros [1,2,3];
- Development of a FEM formulation to model FSI between liquid and tank by FEM model of tank shell and roof, as well as a FEM model of contained liquid as a degenerated solid; Evaluation of time history responses to a given earthquake, including general mapping of stress resultants and generalized displacements, as detailed by Barros and Alves [6] and Barros [3].

One possible approach for predicting the seismic response of storage tanks is based on assuming small liquid displacements. A rigorous mathematical treatment involves deriving an expression for the harmonic fluid velocity potential function $\phi(r,\theta,z,t)$ satisfying Laplace's equation of the BVP expressed in cylindrical coordinates, and also satisfying appropriate boundary conditions at the rigid tank bottom, at the liquid interface with the elastic thin shell, and at the free surface. This velocity potential function may be decomposed into two parts (impulsive and convective) that permit to describe the corresponding effects on the tanks and their performances. The impulsive response is due to the impulsive pressures associated with inertia forces produced by impulsive accelerations of tank wall; while the convective response is due to convective pressures produced by oscillation (sloshing) of the liquid. Figure 3 visualizes these two types of tank responses, induced by earthquake horizontal ground motions.

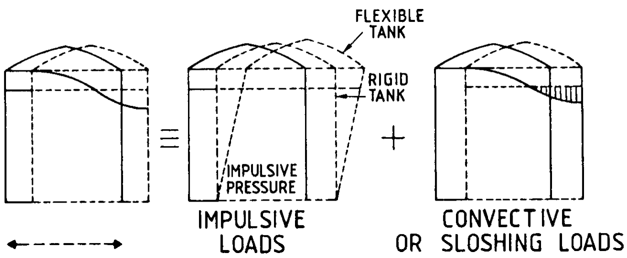

Figure 3: Impulsive and convective tank responses

Through a recent R & D project proposal entitled *Seismic Analysis and Design of Lifeline Structures*, it is expected to further develop the before-mentioned thematic, addressing lifelines infrastructures (tanks, pipelines, bridge piles, among others), as well as evolving through the emerging possibilities of the field of intelligent structures with control devices, permitting to mitigated earthquake and vibration hazards through vibration control [3].

4. SEISMIC RESPONSE OF ANCHORED TANKS BY THE F.E.M.

The following sections detail two methodologies to obtain comprehensive seismic response of tanks under artificial or real earthquakes, according to Portuguese seismic standards for soil type I and zone A with higher seismic risk (A.S. 1-I ; A.S. 2-I).

4.1 Solution of the BVP of the Liquid and FEM Modeling of Tank Shell

The forced vibration of the tank-fluid model is governed by the following variational formulation of Hamilton's principle [1,2,4,5]

$$\delta I = \delta \int_{t_1}^{t_2} (T_t + T_f - U_t + W)\, dt = 0 \tag{1}$$

in which T_t is the kinetic energy of the tank wall, T_f is the kinetic energy of the contained liquid, U_t is the potential strain energy stored in the tank wall, and W is the work done by external loads. (When $W=0$, the variational principle governs free vibration). The velocity potential function is used to obtain the kinetic energy function T_f of the liquid.

Due to the axi-symmetry of the tank fluid-system, once the surface loadings (q_z, q_θ, q_r) are represented in series of harmonic components

$$\left.\begin{aligned} q_z &= \sum_{m=0}^{\infty} \bar{q}_z^{(m)}(z,t)\ \cos m\theta \\ q_\theta &= \sum_{m=0}^{\infty} \bar{q}_\theta^{(m)}(z,t)\ \sin m\theta \\ q_r &= \sum_{m=0}^{\infty} \bar{q}_r^{(m)}(z,t)\ \cos m\theta \end{aligned}\right\} \tag{2}$$

then the shell displacements (u,v,w) would be harmonic of similar forms, in such a way that the m^{th} harmonic component of the displacements is coupled only to the m^{th} harmonic of the loading functions.

But because fluid is assumed inviscid, for all the harmonics it is found that $\bar{q}_z^{(m)}(z,t) = \bar{q}_\theta^{(m)}(z,t) = 0$. The fluid velocity potential satisfying Laplace's equation and boundary conditions is also harmonic, and the m^{th} harmonic of radial loading is expressed in terms of fluid mass density by $\bar{q}_r^{(m)}(z,t) = -\rho_f\ \dot{\varphi}_m(R,z,t)$. For the tank subjected to any horizontal earthquake of ground acceleration $a_g(t)$ through the rigid bottom plate, Figure 4 justifies trigonometrically the existence of the indicated components in the radial and circumferential directions.

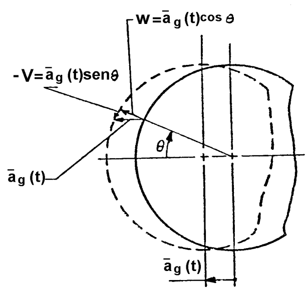

Figure 4: Horizontal harmonic seismic components

Then, only the first ($m=1$) harmonic of tank is excited, because the component $\cos\theta$ is already the trigonometric expansion of itself. Also only the first harmonic term of the hydrodynamic velocity potential will be different from zero. The acting hydrodynamic pressures on the tank walls are then $p = -\rho_f\ \dot{\varphi}(r=R,t)\ \cos\theta$. Uncoupling the BVP by separation of variables permits to express the potential in a series of contributions or terms of Bessel function J_1, as:

$$\phi = \sum_n J_1(\varepsilon_n \frac{r}{R})[\frac{2R}{(\varepsilon_n^{\ 2} - 1)\, J_1(\varepsilon_n)}\ \dot{w} + A_n(z,t)] \tag{3}$$

in which the ε_n are the roots of the Bessel function J_1 of first type and first order, and $A_n(z,t)$ are cumbersome contributions of the interaction between the fluid and the flexible tank wall, detailed by Barros [7].

The tank wall is considered as a linear, elastic thin shell, in which the three-dimensional generalized displacement components (*u,v,w*) are related to the radial, circumferential and axial coordinates (r, θ, z) of a point on the shell middle surface. Neglecting rotatory inertia, the equilibrium equations of Sanders shell theory have already been outlined by Barros [1,2,5]. Standard kinematics relations for membrane strains and curvatures in flexure and torsion, expressed in terms of generalized displacement components (*u,v,w*), are related to the membrane actions $N_z, N_\theta, N_{z\theta}$ and moments $M_z, M_\theta, M_{z\theta}$ represented in Figure 5.

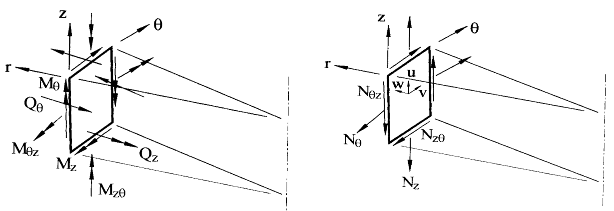

Figure 5: Membrane actions $N_z, N_\theta, N_{z\theta}$ and moments $M_z, M_\theta, M_{z\theta}$ in Sanders theory

The hydrodynamic actions on the shell tank wall depend on the response of the shell and liquid contents to the seismic motions of the foundation soil. Formulating the fluid velocity potential in terms of nodal displacements, the hydrodynamic pressures, the effective generalized forces and the consistent mass and stiffness matrices will also be expressed in terms of full set of nodal displacements.

The finite element model is obtained dividing the tank wall and the contained liquid into ring-shaped finite elements of high b, represented in Figure 6.

The shell displacements for the ring finite element *i*, are:

$$\{d\}^{(i)} = \begin{Bmatrix} u \\ v \\ w \end{Bmatrix}^{(i)} = \sum_m \begin{bmatrix} \cos m\theta & 0 & 0 \\ 0 & \sin m\theta & 0 \\ 0 & 0 & \cos m\theta \end{bmatrix} \begin{Bmatrix} U_m(s,t) \\ V_m\ (s,t) \\ W_m\ (s,t) \end{Bmatrix}^{(i)}$$

$$= \sum_m R_m\ \{A\}_m^{(i)} \tag{4}$$

Also, the vector of amplitudes of m^{th} displacement harmonic for finite element *i* is expressed in terms of the generalized coordinates $\{\alpha\}_m^{(i)}$ by

$$\{A\}_m^{(i)} = D\{\alpha\}_m^{(i)} = \begin{bmatrix} 1 & s & 0 & 0 & 0 & 0 & 0 & 0 \\ 0 & 0 & 1 & s & 0 & 0 & 0 & 0 \\ 0 & 0 & 0 & 0 & 1 & s & s^2 & s^3 \end{bmatrix} \{\alpha\}_m^{(i)} \tag{5}$$

based on assuming that the displacements *u* and *v* are linear (in *s*) while the radial displacements *w* are a polynomial of the 3rd degree (in *s*), as mentioned by Ugural [8].

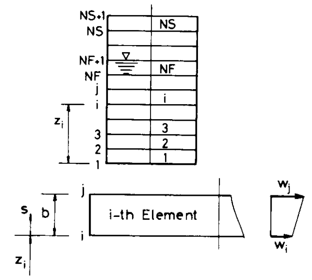

Figure 6: Finite element numbering and local coordinates for individual element

The vector of generalized nodal displacements, at bottom (*s=0*) and top (*s=b*) element ends, is expressed in terms of the generalized coordinates by the following expression in FEM notation for geometric matrix **B** which has already been detailed by Barros [2,5]:

$$\{X\}_m^{(i)} = \begin{Bmatrix} U_m(s=0) \\ V_m(s=0) \\ W_m(s=0) \\ W_{m,s}(s=0) \\ U_m(s=b) \\ V_m(s=b) \\ W_m(s=b) \\ W_{m,s}(s=b) \end{Bmatrix} = B\{\alpha\}_m^{(i)} \tag{6}$$

The generalized coordinates are then

$$\{\alpha\}_m^{(i)} = B^{-1}\ \{X\}_m^{(i)} \tag{7}$$

with which the generalized strains and stresses have been determined [5] using standard FEM notation. Also the (8x8) stiffness matrix of the m^{th} harmonic of generalized displacements of i^{th} element is expressed, in terms of the strains-displacements matrix **C** and material matrix **E** , by:

$$[K]_m^{(i)} = \frac{1}{\pi}\ [B^{-1}]^T \left[\int_0^{2\pi}\int_0^b [C_m]^T\ [E]\,[C]_m\ ds\ d\theta\right][B^{-1}] \tag{8}$$

The equivalent nodal forces are also expressed by

$$\{F\}^{(i)} = \{F\}_1^{(i)} = [B^{-1}]^T \int_0^b (-\rho_f\ \dot{\varphi}) \begin{Bmatrix} 0 \\ 0 \\ 0 \\ 0 \\ 1 \\ s \\ s^2 \\ s^3 \end{Bmatrix} ds \tag{9}$$

since only the first harmonic of the hydrodynamic solution of the velocity potential is non-null. In equation (9) the time derivative of the velocity potential is expressed by a laborious series development in terms of the Bessel function of the first kind and first order and other terms [7], in accordance with the already mentioned equation (3).

However this series development is conveniently truncated after the N most significant terms (usually 5-8 terms suffices, with a truncation relative error less than 0.1%).

Also the consistent mass matrix of the tank i^{th} element is

$$[M]^{(i)} = \rho_s [B^{-1}]^T \left[\int_0^b [D]^T [D] ds \right] [B^{-1}] \tag{10}$$

and the hydrodynamic load vector on the tank shell is expressed by the first N terms truncated from the complete series of Bessel functions by

$$\{F_f\} = -\rho_f [B^{-1}]^T \sum_n J_1(\varepsilon_n) \dot{K}_1^{(n)} \{\beta_1\}_{(n)} \tag{11}$$

where the hydrodynamic quantities $\dot{K}_1^{(n)}$ and the vector $\{\beta_1\}_{(n)}$ have been detailed by Barros [7].

Assembling the finite elements contributions into the global system of equations modeling the coupled fluid-tank shell behavior, neglecting damping one gets:

$$[K]\{V\} = -[M]\{\ddot{V}\} - [M_f]\{\ddot{V}\} + \{F_f\} + \{F_{s,ext}\} \tag{12}$$

where K and M are respectively the global stiffness and consistent mass matrices of the (metallic) tank shell wall. M_f is an effective (or virtual) mass matrix corresponding to the added mass contributions of the tank-contained liquid due to the presence of the fluid near the tank walls. (with non-null terms associated with the radial displacements of the generalized relative displacements vector V), and $F_{s\ ,\ ext}$ is the vector of external applied loads on the tank walls.

The differential matrix equation of motion (12) is conveniently solved applying the Runge-Kutta numerical integration method of 4th order. A computer program was developed (STTKEQ2D.for) that models the above-mentioned formulation. Barros [5] performed a very successful validation of the developed software, for the steel tank represented in Figure 7 completely filled with water and subjected to the so-called Veletsos's pulse.

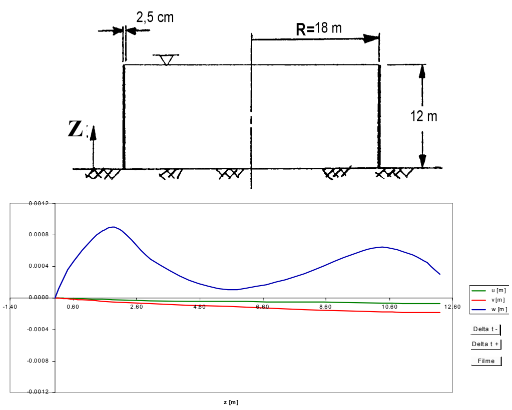

Figure 7: Tank and displacements response to Veletsos's pulse, used to validate model and software

Barros [7] detailed the expressions for the velocity potential and hydrodynamic pressures induced by horizontal earthquakes, permitting to evaluate the total pressures, stresses and displacements and even free surface elevation throughout the tank, according to the Portuguese design standards for seismic actions of types 1 and 2 (AS-1; AS-2). Conceptually, seismic action AS-1 corresponds to a moderate earthquake at short focal distance with 10 seconds duration, while seismic action AS-2 corresponds to a strong earthquake at longer focal distance with 30 seconds duration.

The tank of Figure 7 was subjected to artificial synthetic earthquakes, generated under specific spectrum for the space and temporal evolution of the instantaneous spectral density $S_p(f)$. The strong motion software SIMQKE-II [9] was used herein to produce conditioned or unconditioned earthquake ground motions, matching the target spectrum on average.

Some tank responses to a generic earthquake acceleration time-history were calculated with the developed software STTKEQ2D, and are represented in Figures 8-11 for certain time-steps of the response history. The quantities represented are respectively: the instantaneous axial-shear-membrane stresses, the instantaneous slope of the shell wall, the instantaneous surface elevation, and the time-history of radial displacement at the level of the 4th ring finite element.

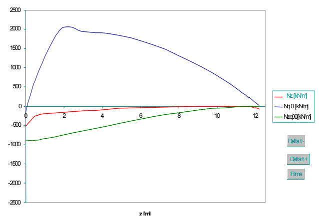

Fig. 8: Axial-shear-membrane stresses

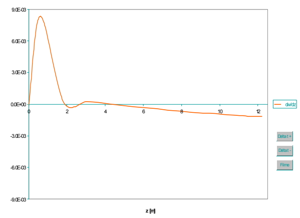

Fig. 9: Slope of shell wall

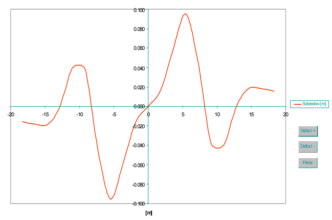

Fig. 10: Surface elevation

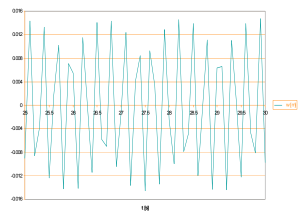

Fig. 11:Radial displacement

Since distinct artificial earthquakes produce distinct families of responses, the question is how many earthquakes need to be generated to determine response envelopes. Limiting the maximum ground accelerations at tank site on soil type I by the spectral density of accelerations specified in Portuguese standards for zone A and seismic actions AS-1 and AS-2, a numerical study was performed for a series of critical values of tank responses [1,2,3]. Convergence was achieved on both average and standard deviation results — of basal moment, basal shear, and slope of the shell wall at the level of the first ring finite element — with a small relative error bound mostly below 3% when the number of earthquakes approaches 14. Convergence was achieved for the amplitude of surface elevation with relative errors below 2%, when the number of earthquakes already reached 10.

With this essential information and with the expression for hydrodynamic pressures [7], the envelopes of hydrodynamic pressure in the given reference tank were obtained for seismic actions AS-1 and AS-2 [1,2,3], as represented in Figure 12. Several other envelopes can be determined for different tank design variables through the developed versatile software, very useful in ascertaining tank design under the strength stiffness and stability viewpoints.

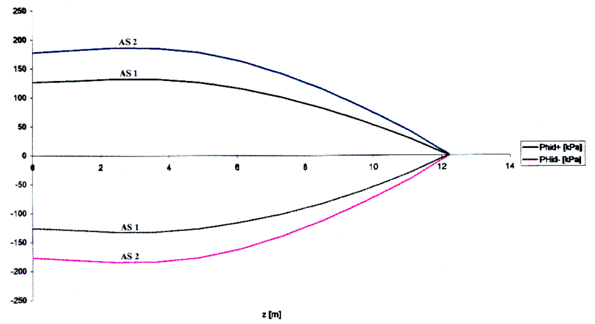

Figure 12: Envelope of hydrodynamic pressures in the reference tank (kPa)

The significant envelope of axial stresses N_z is crucial in evaluating potential onset of elephant-foot bulge buckling, as was applied and explained recently by Barros [2,3,6].

4.2 FEM Solution of the Flexible Tank Coupled with Contained Liquid, by Degenerated Solid Modeling of the Liquid Contents

A second finite element formulation was also developed, for the numerical and computational modeling of tanks with and without sloshing of contained liquid. The tank wall and roof are modeled with 8-noded isoparametric elements derived from the classical formulation of Ahmad [6]. The Reissner-Mindlin hypothesis of thick shell theory is considered in a Green's deformation field, with shear-locking effects eliminated as explained in [6]. Ring stiffeners are modeled with 3-noded Timoshenko beam elements, with reduced integration. The stiffening rings are rigidly welded in the tank's exterior eccentrically placed relative to the thin shell middle surface. To evaluate their effect in the tank seismic analysis, the beam element nodes are considered to be slave (or dependent) nodes in relation to the shell nodes, by means of appropriate geometric transformation matrices. The contained liquid is represented by degenerated elastic solid elements constituting a practical means of addressing fluid-structure interaction. In this manner, a finite element mesh with hexahedral elements of 20-nodes discretizes the liquid. To avoid the occurrence of singular matrices it is considered that the shear modulus G→0, but not null, related with the elastic modulus E and Poisson ratio ν by $G=E/[2(1+\nu)]$. Also, contained liquid incompressibility (namely, water) is simulated with a Poisson ratio ν close to 0.5 (in practice, ν →0.5), also linked to the previous criteria. As the contained liquid bulk modulus of volumetric elasticity is given by $K_v=E/[3(1-2\nu)]$, the values of E and ν to be used in the seismic tank analysis should be mutually adjusted to obtain for K_v the appropriate bulk modulus of the contained liquid. To obtain simultaneously the conditions G = 0 MPa and K_v = 2.11 GPa it is possible to consider a multiplicity of pairs (E, ν) that would numerically satisfy these conditions. The properties E = 0.0633 MPa and ν = 0.499995 (→ 0.5, as required) were adopted herein, leading to K_v = 2.11GPa and G = 0.0211 MPa (→ 0, as required). To exemplify its applicability the seismic response of a tank is briefly presented, for a given time-record of a synthetic earthquake.

The steel tank studied has an outside diameter of 36 m and a height of 12 m, and is filled with water up to a height of 10 m as represented in Figure 13. It is rigidly connected to the ground and designed according to the Japanese standard JIS B-8501 with a thickness of 8 mm throughout. The stiffening ring, strengthening the roof support on the shell wall at the top, is an angle (L 90x90x9) with equal flanges.

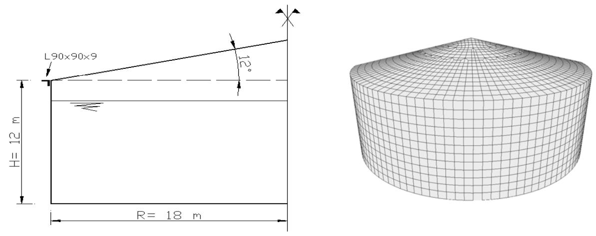

Figure 13: Tank studied and its finite element mesh

Some natural frequencies and mode shapes of the complete structure are presented (Figure 14), as well as instantaneous deformed shapes (Figure 15) and envelopes of shell stress resultants (Figure 16).

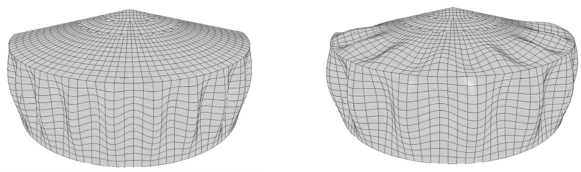

ω_{12} =27.07 rad /s ω_{32} =35.22 rad /s

Figure 14: Some natural frequencies and mode shapes of the complete tank

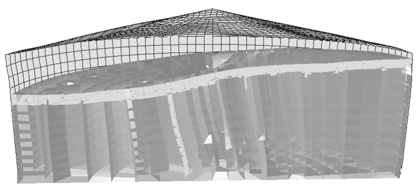

Figure 15: Deformed shape and sloshing at t=9.24s

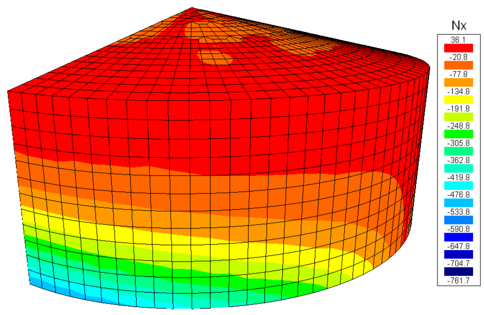

Figure 16: Vertical compression of the shell along tank wall (kN/m)

The stress envelope can be used in conjunction with critical buckling stress of symmetric instability of cylindrical shells in function of the order of the harmonic, to ascertain the minimum design thickness requirements used (Barros et al. [6]), by assessing the ultimate capacity by instability of the laminar structure of the tank walls near the base.

5. ACTIVE CONTROL OF PIPELINE-CYLINDERS UNDER FLEXURAL VIBRATIONS

Active control of structural vibrations has received considerable attention in recent years. Due to the size and massiveness of civil engineering structures, vibration control by point forces of piezoelectric origin is impractical. However piezoceramic actuators can develop much higher forces, without any reaction mass.

Herein is briefly described some methodology for vibration control in tube-like structures — namely pipelines, aeronautical-astronautical fuselages or submarine structures — through piezoceramic stacks of actuators. Based on available literature and also on Barros [3], the general idea is that of using the flange of existing ring stiffeners, in tube-like structures, as support for a stack of piezoceramic control actuators between the shell and the ring, as represented in Figure 17. Notice however that this idea can be easily extensible to other general situations of vibration control.

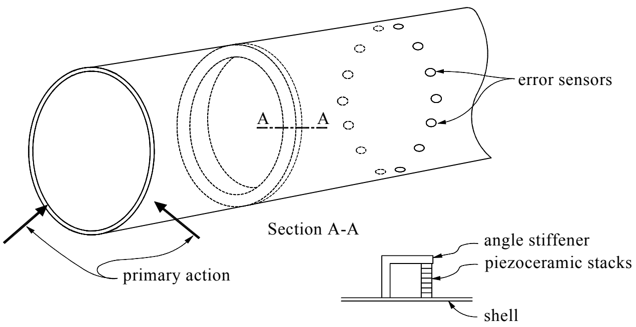

Figure 17: Vibration control on cylinders by piezoceramic stacks of actuators

For the analytical study consider a perfect cylinder under general 3D harmonic excitation $q(x_0, \theta_0)$ in longitudinal or axial x-direction, in circumferential or tangential θ-direction and in radial r-direction (Figure 18).

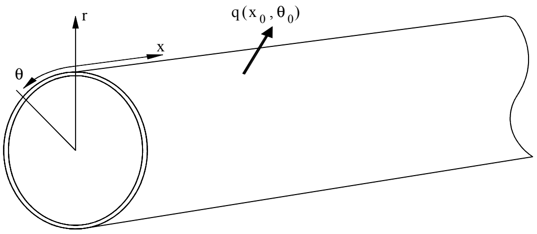

Figure 18: Cylinder with general 3D harmonic excitation

Flugge's shell theory with inertia terms is now used since it simplifies Sanders's theory (Leissa [10]). Solution of Flugge's equations of free motion is expressed in terms of a harmonic series of eigenfunctions, and also modal wave numbers, characterising the circumferential mode shapes.

For a tubular pipeline under a point force or a point moment, the cases of simply supported (SS) boundary conditions and SS plus semi-infinite have been analytically studied [3]. Also for modelling the effect of a ring angle stiffener at a section distinct from the section of point actions, three (eigen) functions solutions of Flugge's equations of motion were determined in radial direction [3].

Control is achieved through added effects of point forces on actuators and generalized forces (reaction line force and line moment) in the ring at base of stiffener. The displacement field in any point results from displacements due to primary excitation (source action) and from displacements due to control forces and moments (control source). The optimal control criterion consists in minimising the total mean square displacements at discrete points in a ring of sensors (proving ring or error sensing ring).

6. CONCLUSIONS

Two FEM approaches were used to analyse seismic response of liquid-filled tanks and to determine design envelopes, through successfully validated software. Analytical study on vibration control in tube-like structures was briefly outlined.

References

[1] **Barros, R.C.**, Seismic Response Envelopes of a Bottom-Supported Tank, *Proc. 6th Int. Conf. on Computational Structures Technology*, Civil-Comp Press, Prague, September 2002 (*in press*).

[2] **Barros, R.C.**, Resposta Sísmica de Tanques de Armazenamento de Líquidos, *Contents of the Synthesis Lecture of the Aggregation Evaluation in Civil Engineering*, Department of Civil Engineering, FEUP, Porto, 5th July 2000, (*in Portuguese*).

[3] **Barros, R.C.**, Some Developments on Vibration Control for Tank Shells and Pipelines, *Oral presentation* on 25th September 2001 in the *Engineering Meeting on Intelligent Structures*, Ischia, Italy, 2001.

[4] **Haroun, M.A.**, Dynamic Analyses of Liquid Storage Tanks, *Report to the National Science Foundation*, EERL 80-04, California Institute of Technology, Pasadena, 1980.

[5] **Barros, R.C.**, Modelação da Resposta Sísmica de Tanques Circulares pelo M.E.F., incluindo Interacção Tanque-Líquido, *Proc. VI Congresso Nacional de Mecânica Aplicada e Computacional*", Vol. 2, pp. 1203-1212, Lisboa, 2000, (*in Portuguese*).

[6] **Barros, R.C., Alves, R.F.**, Seismic Response of Metallic Storage Tanks by Degenerated Solid Modeling of the Liquid Contents, *Engenharia: Estudo e Pesquisa*, Vol. 4, No. 2, pp. 71-77, Brazil, 2001.

[7] **Barros, R.C.**, Pressões Hidrodinâmicas nas Paredes, Esforços e Deformações Generalizadas em Tanques Circulares Apoiados no Solo e Sujeitos à Acção Sísmica tipo 1 e 2, *Research Report* of Project PRAXIS XXI nº ECM/10250-98/P, Dept of Civil Engineering, FEUP, Porto, Portugal, 2002, (*in Portuguese*).

[8] **Ugural, A.C.**, Bending Stresses in Shells, *Stresses in Plates and Shells*, Ch. 11, pp. 231-253, McGraw-Hill Book Company, New York, 1981.

[9] **Vanmarcke, E.H., Fenton, G.A., Heredia-Zavoni, E.**, SIMQKE-II: Conditioned Earthquake Ground Motion Simulator, User's Manual, Version 2.1, Princeton University, Princeton, New Jersey, 1999.

[10] **Leissa, A.W.**, Vibration of Shells, *NASA SP-288*, USA, 1973.